

Short Communication

Fabrication and Characterization of Ferrocene Containing Hydrogel for Glucose Biosensor Application

Bruno R. Crulhas, Naira P. Ramos, Caroline R. Basso, Vladimir E. Costa, Gustavo R. Castro, Valber A. Pedrosa*

Institute of Bioscience, UNESP, Botucatu, SP – Brazil

*E-mail: vpedrosa@ibb.unesp.br

Received: 2 September 2014 / Accepted: 14 October 2014 / Published: 28 October 2014

A detailed electrochemical study of a novel microsystem biosensor based on ferrocene (Fc) intercalated poly(ethylene) glycol (PEG) and its potential use in the development of amperometric biosensors is presented. A redox hydrogel electrode, fabricated by covering the PEG-FC on the surface of gold microelectrode, exhibits a quasi reversible electrochemical characteristic. The characterization and dependence of Fc concentration to construct the biosensor were carried out by cyclic voltammetry measurements. The sensitivity, repeatability and linearity of the new glucose biosensor are found to be excellent over earlier reported glucose biosensor.

Keywords: Biosensor, glucose detection, redox mediator

1. INTRODUCTION

In past years, microfluidics systems had attracted interest due to their properties, such as: need small quantities of sample for analyzing, limit reagent use and high sensitivity especially in biotechnology fields involving biosensor. Enzyme-based electrodes are an important class of biosensors where we can detect byproducts of enzymatic breakdown [1,2]. Enzyme-based sensor has been used to monitoring a variety of diseases such as diabetes, cardiac biomarker and cancer by detecting energy metabolites [3,4,5]. These microsensors have an increased detection sensitivity, specificity and multiplexing capability on portable devices for use in several areas. Reduced reagent consumption significantly lowers costs, which is an important concern in clinical laboratories. All these benefits make microfluidics technology ideal for point-of-care testing [6,7,8].

The discussion of the mechanism of electron exchange from enzymes that governs sensor performance is an important field of biosensor mode. There are number of articles, reviews, books,

patents available on biosensors providing specific details of electron exchange mainly through three main modes; (1) non-mediated; (2) mediated and (3) electrocatalytic. More specific measuring glucose is continuously under development using microsystems. Recently, a new approach for creating microbiosensors involves electrodeposition of a conductive hydrogel polymer [9,10,11]. Hydrogels are attractive materials in microfabrication electrochemical biosensors because it provides an excellent matrix for enzyme encapsulation [12]. Several researches have used a uniform gel membrane coated on top of the microfabricated electrodes to prevent fouling and enzyme leaching [13], whereas far fewer reports describe the integration of patterned gel layer with electrodes [14]. Recently, Yan *et al.* 2010 [15], manufactured a biosensor with poly(ethylene) glycol (PEG) hydrogel. There is a preference for PEG instead others polymers, because it possess a broad range of properties, making them attractive for biosensor fabrication. PEG hydrogels are an excellent matrices for entrapment of biomolecules [16,17]. These hydrogels are non-fouling and can therefore help eliminate biosensor fouling in complex solutions such as physiological fluids or cell culture media [18,19]. In addition, it can be micropatterned in a process similar to photolithography and are semiconductors [20].

However many of these works used soluble redox mediator which introduce additional complications while use of oxygen is also often unsatisfactory for measure in flowing systems. To overcome this problem we verified how the inclusion of ferrocene (redox molecules) could enhance electron transfer through hydrogel and calculated optimum ratio of ferrocene (Fc), polymer, and enzyme to avoid destabilizing the sensor and achieve a better electrochemical signal. The strategy for integrating redox molecules into hydrogels onto miniature electrodes described in this paper should be broadly applicable in construction of robust and sensitive enzyme-based biosensors.

2. EXPERIMENTAL PROCEDURE

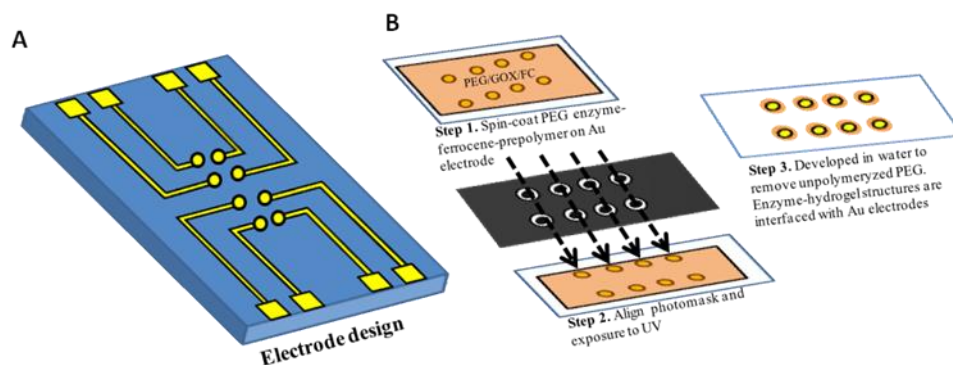
2.1 Chemicals and Reagents

Poly(ethylene)glycol diacrylate (PEG-DA, MW 575), 2-hydroxy-2methyl-propiophenone (photoinitiator), 99.9% toluene, Glucose oxidase (EC 1.1.3.4, type II-S from *Aspergillus niger* (18 000 U g⁻¹ solid), Ferrocene, glutaraldehyde, D-(+)-glucose and 3-(trichlorosilyl) propyl methacrylate were purchased from Sigma (St Louis, MO). Phosphate buffer (PBS) 0.10 M was used as an electrolyte for all electrochemistry experiments. Water used for preparation of aqueous solutions came from a Millipore Direct-Q water purification system (resistivity, 18 M Ω cm⁻²). D-(+)-Glucose solutions were allowed to muta-rotate overnight at room temperature before use. Stock solutions were prepared in milli-Q water and stored in the dark at 4 °C.

2.2 Fabrication of Au electrode arrays

Electrode array layout was designed in AutoCAD and converted into plastic transparencies by DGM design (Curitiba, PR). Design of the Au electrode arrays is shown in Figure 1A. Fabrication of gold electrode arrays, were made at Brazilian Nanotechnology National Laboratory (LNNano/CNPEN, Campinas/SP), we sputter-coated standard (75 mm \times 25 mm) glass slides with 15

nm Cr adhesion layer and 100 nm Au layer. Electrodes were fabricated using traditional photoresist lithography and wet etching processes. Etching of Au/chrome layers resulted in an array of eight working microelectrodes patterned on a glass slide. Each Au electrode was 300 μm in diameter with 15 μm wide leads and 1 mm \times 1 mm square contact pad (see Scheme 1A for layout of electrodes).



Scheme 1. (A) Layout of an electrode array consisting of eight Au electrodes. (B) Micropatterning enzyme-carrying hydrogel microstructures in Au electrodes.

2.3 Functionalization of electrodes substrates

For improving hydrogel adhesion on electrode substrate electrodes were modified with 3-(trichlorosilyl) propyl methacrylate. Glass surfaces were silanized as following standard protocol [21]. Briefly, glass slides were cleaned in “piranha” solution consisting of 3:1 ratio of H_2SO_4 and H_2O_2 for 30 minutes, washed in mili-Q water and subsequently immersed in 2 mmol L^{-1} toluene solution of 3-(trichlorosilyl) propyl methacrylate (TPM) for 1 hour to obtain a self-assembled monolayer of silane on glass regions then substrates were washed in toluene to remove excess of silane agent and finally were placed in an oven for 3h at 100°C to crosslink the silane layer.

2.4 Integration of Au Electrodes with Enzyme-Carrying Hydrogel Microstructures

When preparing enzyme electrodes, to testing the influence of different concentrations of Fc, we used five different concentrations (2.5 mg/mL, 5.0 mg/mL, 10.0 mg/mL, 15.0 mg/mL and 20.0 mg/mL). GOx was dissolved in PBS buffer (pH 6.0) to reach concentration of 20 mg/mL and glutaraldehyde was added to enzyme solution at 2.0% v/v to improve enzyme retention and function of the biosensor.

Prepolymer solution was prepared by adding 2.0% (v/v) of photoinitiator (2-hydroxy-2-methylpropiophenone) and Fc to PEG-diacrylate (DA) (MW 575). Enzyme and prepolymer solution were combined by adding 0.1 mL of the enzyme solution to 0.4 mL of PEG-DA/ferrocene. Mixture was stirred for 4 hour at 4°C to ensure homogeneous dispersion of enzyme molecules.

In the next step, PEG prepolymer solution containing enzyme molecules and redox species was photopolymerized on top of the Au electrodes in a process similar to photolithography (see Figure 1B). Briefly, PEG-based prepolymer solution was spin-coated at 800 rpm for 4 s onto glass slides

containing Au electrode patterns. A photomask was made with an electrode pattern and then exposed to unfiltered UV light at 70 mW/cm^2 for 10 s to convert liquid prepolymer into cross-linked hydrogel. Surfaces were developed in milli-Q water to remove unpolymerized PEG precursor solution. Enzyme carrying hydrogel microstructures were made larger than Au electrodes, 600 and 300 μm diameter for hydrogel and Au features, respectively. This was done to ensure effective anchoring of the polymer structures to silanized glass substrate. To help visualize deposition of the polymer microstructures on adjacent electrodes, we utilized an optical microscope coupled with a digital camera (Figure 2).

2.5 Electrochemical Characterization and Functionalization of Enzyme Electrodes

Electrodes were tested in a custom-made, Plexiglas electrochemical cell with a volume of ~ 1 mL and PBS (pH 6.0). Two electrochemistry techniques: cyclic voltammetry and spectroscopy impedance were used to characterize the sensor response to glucose and lactate. D-Glucose solutions were stored overnight at room temperature to allow equilibration of the α and β -forms. To characterize redox properties of ferrocene-containing hydrogel, we used cyclic voltammetry with scan rates ranging from 20 to 250 mV/s.

2.6 Equipments

Voltammetric and spectroscopy impedance experiments were performed using a μ Autolab Type III/response analyzer (Metrohm Autolab) with a frequency range of 100 kHz–100 mHz and signal amplitude of 5 mV. Experiments were conducted in a three electrode system containing a counter electrode wire of titanium coated with platinum, a saturated Ag/AgCl (3 M) reference electrode and enzyme-modified working electrode. All electrochemical measurements were performed at room temperature.

3. RESULTS AND DISCUSSION

3.1 Surface Modification and Fabrication of Au electrodes

In previous publication we described the use of enzyme-carrying hydrogels for development of electrochemical biosensor using gold nanoparticle to enhance conductivity of PEG hydrogel [12]. Conjugation of GOX molecules to AuNP and encapsulation of these conjugates in PEG hydrogel microstructures allowed constructing biosensor with glucose higher sensitivity. These remarkable observations further directed our attention to study the following: (1) dependence of ferrocene on kinetics of bioelectrocatalysis; and (2) effect of concentration substrate permeability in these films.

An overview of electrode arrays is shown in Figure 1A. The device consisted of an array of 2 x 4 electrodes with 300 μm diameter connected to contact pads via 10 μm wide leads. Following fabrication of Au electrodes, substrates were modified with methacrylate silane agent to secure

covalent attachment of PEG hydrogel to glass (Figure 1B). Silanization did not influence the electrochemical experiments as we see the results below.

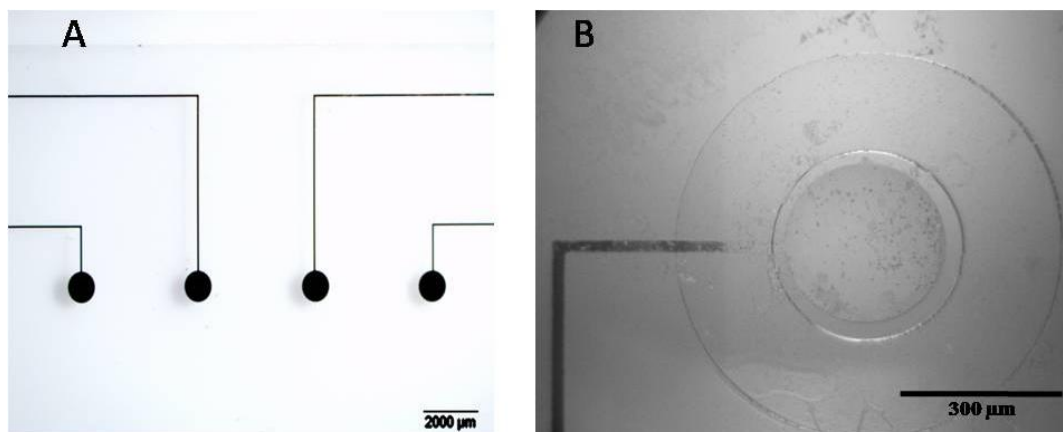


Figure 1. (A) Portion of eight-electrode array. (B) PEG-Fc enzyme microstructures polymerized around the Au electrode.

3.2 Enhancement of Charge Transport in Ferrocene-PEG Hydrogels

Typical cyclic voltammograms of PEG-Fc cross-linked on the gold electrode in PBS buffer solution at pH 6.0 are shown in Figure 2A. As characterized by cyclic voltammetry, immobilizing pure PEG (black line) on top of Au electrodes resulted in effective insulation of the electrodes. Encapsulation of ferrocene show a typical cyclic voltammograms (red line) where redox reaction easily occurred on electrode with anodic peak potential at 0.3 V and cathodic peak potential at 0.09 V vs Ag/AgCl. After 15 cyclic voltammograms, E_{pa} and E_{pc} remained constant. Electrochemical stability of PEG-Fc subjected to several cyclic voltammograms indicates a remaining ferrocene derived electroactive species which cannot diffuse from the hydrogel.

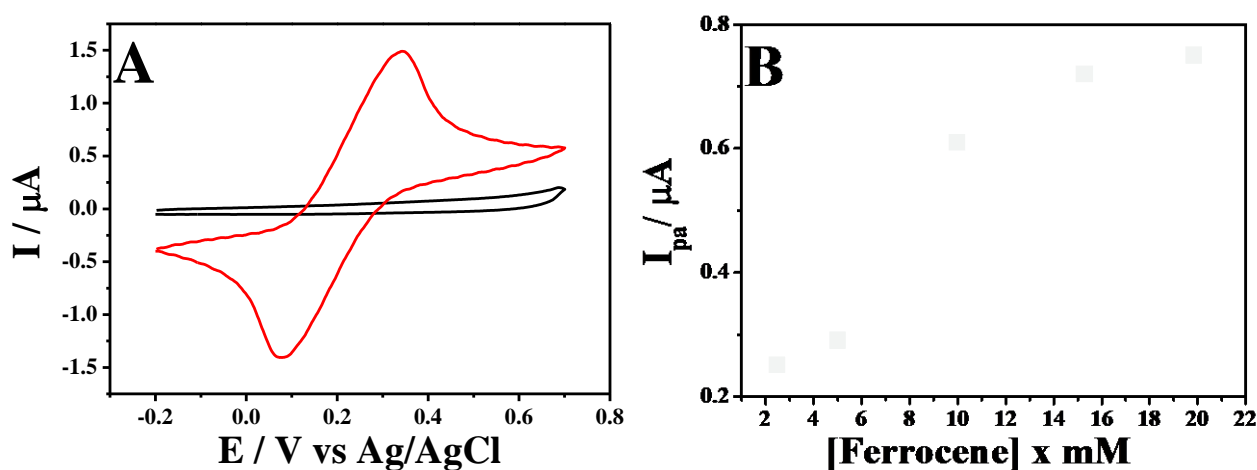


Figure 2. (A) Cyclic voltammograms of PEG-Fc in 10 mM PBS buffer at pH 6.0, scan rate 50 mV/s. (B) Steady-state peak current of PEG vs concentration of Fc in the hydrogel. Cyclic voltammetry was performed in 10 mM PBS buffer from -0.2 to 0.7 V at scan rate 50 mV/s.

We hypothesized that increase of Fc could improve electron transfer of hydrogels. To test this hypothesis electrode arrays functionalized with hydrogels were characterized by cyclic voltammetric. A set of redox hydrogel containing different ferrocene concentration were prepared. Figure 2B shows anodic peak increased with increasing of ferrocene concentration. Optimal concentration of Fc found was 10 mg/mL rather than high concentrations like the usual concentration of 20 mg/mL encountered in several papers [15,21]. This was primarily attributable to the microenvironment of electrode cell; nanofabrication allows use of lower amounts of compounds with an enhanced electrochemical signal response. Despite high concentrations of Fc virtually predicts higher levels of current, using them, PEG-prepolymer solution became more unstable, compromising the cross-link with enzymes and polymer film. Therefore, we used the 10 mg/mL concentration in the subsequent experiments with enzymes.

Figure 3A shows cyclic voltammograms of the PEG-Fc modified electrode at different potential scan rates in order to investigate the kinetics of the electrode reactions. Results demonstrated oxidation and reduction peaks occur at 0.1V and 0.3V, respectively, with linear equation of $I_{pa} (\mu A) = 0.56 + 0.27 (mV/s) (R=0.9994)$. Increase in peak current is proportional to square of potential scan rate which indicating that the charge transfer may be described by the Randles-Sevcik equation [22], and point out a determining step of reaction is controlled by mass transport. Our results are similar with literature values [20]. Hydrophicity of PEG and ferrocene resulted in a hydrogel redox polymer structure that promotes facile permeation of the films by substrate and product molecules.

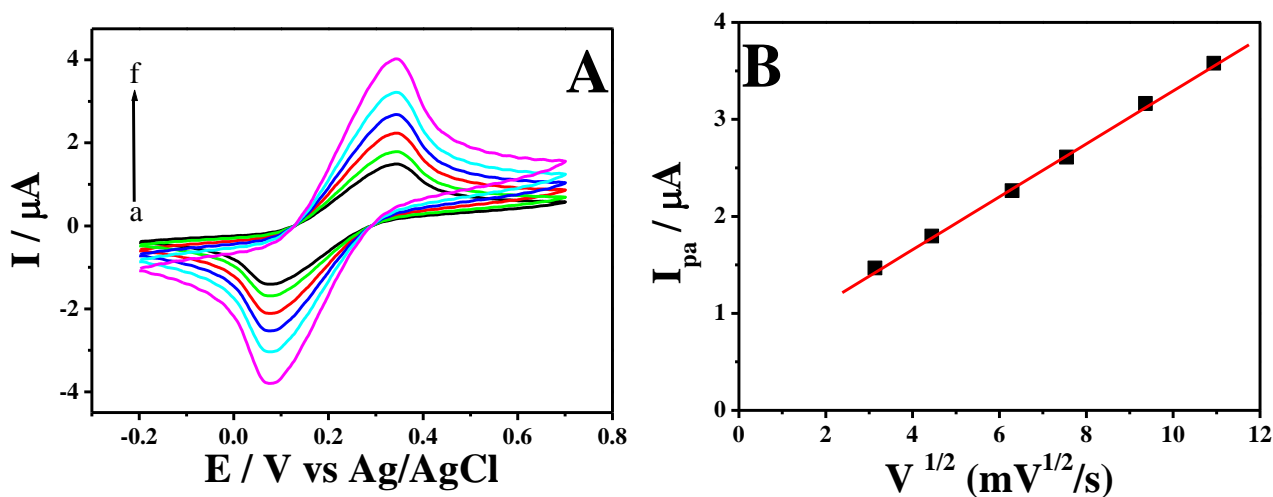


Figure 3. (A) Cyclic voltammograms of the PESCOOH-Au modified electrode at different scan rates (a-i: 20, 30, 50, 60, 90, 100, 150, 200, and 250 mV/s) in 10 mM PBS (pH 4.0) + 10 mM FcMA, and (B) Plot of the redox peak current versus the square root of scan rate.

Furthermore, a linear correlation was obtained between peak potential and logarithm of the scan rate. For a mass controlled process, charge transfer coefficient (α) and apparent heterogeneous electron transfer rate constant (k_s) can be calculated from variation of E_{pa} and E_{pc} with logarithm of scan rate (Figure 4) follows the Laviron's model. One linear regression equations of $\Delta E (E_p - E^{0'})$; E_p is the peak potential value for the anodic or cathodic branch, and $E^{0'}$ is the formal potential) versus log of

the potential scan rate are plotted (Figure 4) and expressed as $E_p (v) = 0.25 \log v + 0.91$ ($r = 0.996$) and using the Laviron's equation. The slope of the linear equation is equal to $\alpha \log(1-\alpha) + (1-\alpha) \log \alpha - \log RT/nFv - (\alpha(1-\alpha)nF\Delta E_p/2.3RT)$ which can be used to evaluate the kinetic parameters, R , T and F are referred to gas, temperature and Faraday constant, respectively. The electron transfer rate constant (k_s) was calculated to be 8.5 s^{-1} using the following Laviron's equation [23]. The calculated k_s value was higher than some reported values [24,25], indicating redox hydrogel modified electrode exhibited fast electron transfer rate towards the electrochemical oxidation of ferrocene.

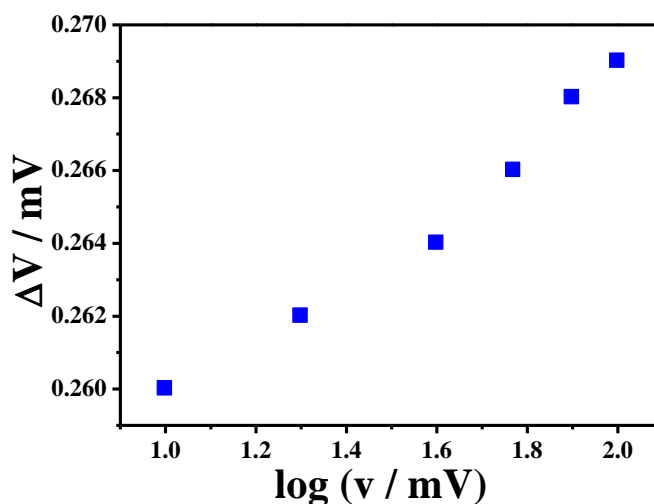
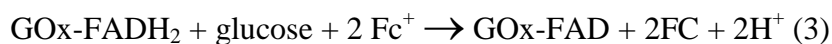


Figure 4. Peak-to-peak separation as a function of the potential scan rate. The measurements were performed in 10 mM PBS buffer (pH 6.0).

After fabricating enzyme-carrying hydrogel/Au Electrodes we characterized biosensor response to the analyte of interest: glucose as seen in Figure 5, the enzymatic reaction releases gluconolactone, and finally electrons are generated into electrochemical cell, improving electric current. The cyclic voltammograms were recorded before and after the addition of glucose. The cyclic voltammograms of has also been recorded as shown in Figure 5A both in absence and presence of glucose. Figure 5A shows change in CV with an increased of current as function of glucose solutions with a major increment at higher concentrations of glucose. Bioelectrocatalytic oxidation was obtained due to oxidation of glucose, equation (1), where GOx-FAD (2) and GOx-FADH₂ (3) represent the oxidized and reduced forms, respectively, of the flavin adenine dinucleotide where bound to the active site of GOx, and Fc represents a ferrocene residue.



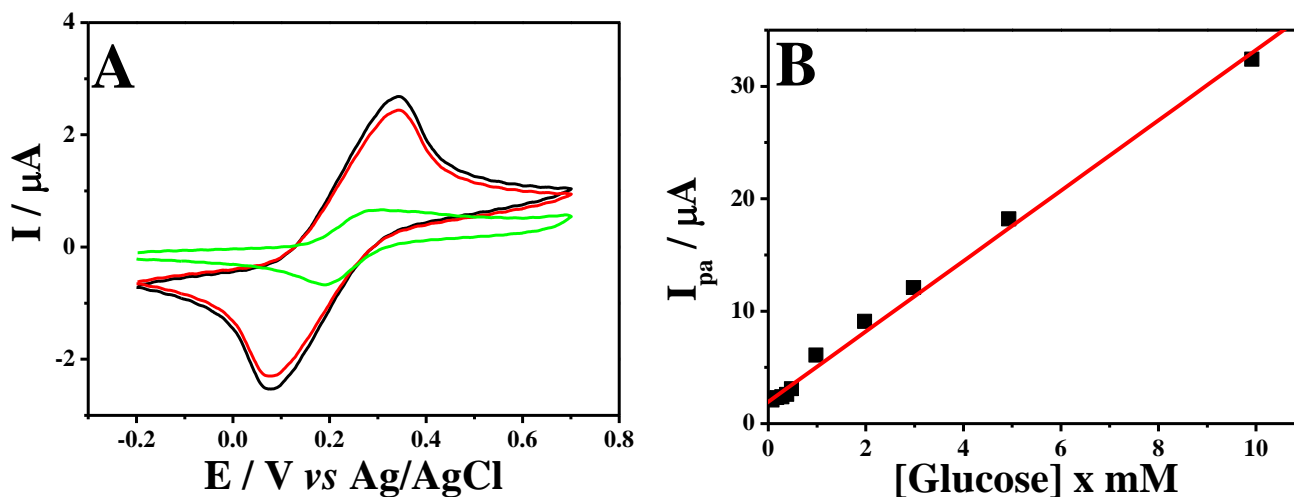


Figure 5. A) Cyclic voltammograms for biosensor, with the optimized parameters. The glucose concentrations in $\mu\text{mol L}^{-1}$ are: without glucose (green line); 0.4 (red line); 0.5 (black line); B) Linear dependence of the peak current with glucose concentration.

Using optimized conditions, Figure 5B shows the response obtained using cyclic *voltammetry* range of concentration 0.1 to 10 mM of glucose solution in 0.1 M pH 6.0 PBS at biosensor. Linear dependence of the I_p vs [glucose] relationship is described by $I_{pa} = 0.004 \mu\text{A} + 0.30 \mu\text{A}/\mu\text{mol L}^{-1}$ [glucose], with a correlation coefficient $R = 0.997$. The detection limit defined as using a $3\sigma/\text{slope}$ ratio, where σ is the standard deviation of the mean value for 10 voltammograms of the blank, was found to be $2.0 \mu\text{mol L}^{-1}$. The repeatability of the response current of the sensor was investigated at a glucose concentration of $0.1 \mu\text{mol L}^{-1}$. The variation coefficient (RSD) was 4.8% for ten successive injections of the same concentration at different times, implying good reproducibility of the biosensor. Also, we performed a series of reference experiments using other common interfering species such as fructose, lactose and uric acid for biosensors operating under physiological conditions regards the fact that the real signal may be masked by interference. A total of 2 mM control samples were investigated and no detectable signals were obtained. The results suggested the proposed biosensor suitability to practical applications.

4. CONCLUSION

Our paper describes an optimized biomaterial microfabrication technique. PEG hydrogel photolithography with ferrocene and glucose oxidase, as an enhanced strategy for development of electrochemical enzymatic sensor. Similar Photolithograph process was used to functionalize Au electrode arrays with enzyme-carrying hydrogel microstructures. The biosensors were characterized electrochemically and the inclusion of ferrocene was found to enhance conductivity of PEG hydrogels but the optimal ratio was found at lower concentration of ferrocene (10 mg/mL). The cross-link of GOx molecules in PEG hydrogel microstructures allowed constructing biosensors with an improved

current and lower detection limit of 2.0 $\mu\text{mol L}^{-1}$. In addition to providing an excellent matrix for enzyme entrapment, PEG hydrogels are nonfouling. The present paper provides an optimization for fabricating miniature enzyme-based electrodes using PEG-Fc as a biocompatible, nonfouling, and can be used to cell-friendly polymer.

ACKNOWLEDGEMENTS

The authors thank FAPESP (2014/05653-3), and CNPq (475328/2013-2), Brazil, for the grants and the financial support to this work.

References

1. Y. Hu, Y. Zhang and G. S. Wilson, *Anal. Chim. Acta* 1993 (1993) 503
2. T. J., Ohara, R. Rajagopalan, A. Heller, *Anal. Chem.* 66 (1994) 2451
3. S. O'Rahilly, A. Vidal-Puig, *Science* 431 (2001) 125
4. A.J.S. Ahammad, Y.H. Choi, K. Koh, J.H. Kim, J.J. Lee, M. Lee, *Int. J. Electrochem. Sci* 6 (2011) 1906.
5. R. A. Gatenby and R. J. Gillies, *Nat. Rev. Cancer* 4 (2004) 891
6. Y. Xiao, F. Patolsky, E. Katz, J. Hainfeld, I. Willner, *Science* 299 (2003) 1877
7. W. Cai, Q. Xu, X. Zhao, J. Zhu and H. Chen, *Chem. Mater.* 18 (2006) 279
8. M. Bui, S. Lee, K. Han, X. Pham, C. Li, J. Choo and G. Seong, *Chem. Commun.* (2009) 5549
9. W. Lee, R. Scholz, K. Niesch, U. Gosele, *Angew. Chem. Int. Ed.* 44 (2005) 6050
10. X. Luo, J. Xu, Q. Zhang, G. Yang, H. Chen, *Biosens. Bioelectron.* 21 (2005) 190
11. W. Chen, C. Li, P. Chen, C. Sun, *Electrochim. Acta* 52 (2007) 2845
12. V. Pedrosa, J. Yan, A. Simonian, A. Revzin, *Electroanal.* 23 (2011) 1142
13. A. Mugweru, B. L. Clark and M. V. Pishko, *Electroanal.* 19 (2007) 453
14. I. Moser, G. Jobst and G. Urban, *Biosens. Bioelectron.* 17 (2002) 297
15. J. Yan, V. Pedrosa, A. Simonian and A. Revzin, *ACS Appl. Mater. Inter.* 2 (2010) 748
16. A. Revzin, R. J. Russell, V. K. Yadavalli, W. G. Koh, C. Deister, D. D. Hile, M. B. Mellott and M. V. Pishko, *Langmuir* 17 (2001) 5440
17. W. G. Koh, M. Pishko, *Sens. Actuators B.* 106 (2005) 335
18. P. D. Drumheller, J. A. Hubbell, *J. Biomed. Mater. Res.* 29 (1995) 207
19. C. P. Quinn, C. P. Pathak, A. Heller, J. A. Hubbell, *Biomaterials* 16 (1995) 389
20. A. Revzin, R. G. Tompkins and M. Toner, *Langmuir* 19 (2003) 9855
21. J. Yan, V. Pedrosa, J. Enomoto, A. Simonian and A. Revzin, *Biomicrofluidics* 5 (2011) 032008
22. T.R.T.A. Antonio, C. R. Basso, M. F. Cabral, V. A. Pedrosa, *Int. J. Electrochem. Sci.* 8 (2013) 4150
23. E. Laviron, L. Roullier, C. Degrand, *J. Electroanal. Chem. Inter. Electrochem.* 112 (1980) 11
24. Z. Huafang, D. Shaojun, *Electrochim. Acta*, 42 (1997) 1801.
25. H. Zhou, S. Dong, *J. Electroanal. Chem.* 414 (1996) 121.